# Some observations in grinding unidirectional carbon fibre-reinforced plastics

N.S. Hu, L.C. Zhang*

*School of Aerospace, Mechanical and Mechatronic Engineering, The University of Sydney, Sydney 2006, NSW, Australia*

## Abstract

This paper investigates the grinding performance of epoxy matrix composites reinforced by unidirectional carbon fibres, using an alumina grinding wheel. Emphasis was placed on understanding the effect of fibre orientations and grinding depths on the grinding force and surface integrity, and on understanding the grinding mechanisms, with a comparison to orthogonal cutting. It was found that greater grinding forces occurred at a fibre orientation between 60° and 90°, but poorer grinding surface finish took place between 120° and 180°. The surface integrity was highly dependent on the fibre orientation and the depth of grinding, which is very similar to the results of orthogonal cutting. © 2004 Elsevier B.V. All rights reserved.

## 1. Introduction

Fibre-reinforced plastics (FRP) have been widely used in industry due to their excellent properties such as high specific modulus, specific strength and damping capacity. Although near-net-shape components can be produced, they usually require a subsequent machining to form the desired geometry, assembling tolerance and surface integrity. Grinding is particularly needed to acquire high dimensional accuracy and surface finish.

Unlike the investigations into the machining of traditional metallic materials, relatively little study has been carried out on machining advanced composite materials; thus the mechanisms are less understood. However, it has been reported that the strong anisotropy and inhomogeneity of FRP introduces many specific problems in machining, such as fibre pullout, delamination, surface damage, burrs and burning.

The investigations into various machining aspects of FRP have been focusing on the issues such as chip formation [1–7] and cutting forces [2,5–7]. For example, Tagliaferri et al. [8,9] investigated the effect of drilling parameters on the cut quality and mechanical behaviour of FRP, discussed the interaction mechanisms between the drilling tool and FRP material, and studied the damage development. Inoue and Kawaguchi [10] investigated the influence of yarn direction on the failure mode and the appearance of the ground surface of the glass FRP. Park et al. [11] investigated the mirror-surface grinding of carbon fibre-reinforced plastics using a micro-grain metal bonded diamond wheel with electrolytic in-process dressing. Recently, Wang and Zhang [12–14] characterised the machining damage in unidirectional FRP subjected to cutting and developed a new mechanics model to predict the cutting forces. Mahdi and Zhang [15,16] presented a two-dimensional cutting model to predict the cutting force in relation to fibre orientations and developed an adaptive three-dimensional finite element algorithm. Zhang et al. [17] investigated the formation of the exit defects in FRP plates caused by drilling and based on a dimensional analysis, proposed a simple formula for damage prediction.

This paper aims to acquire a better understanding of the surface grinding of unidirectional carbon fibre-reinforced plastic components.

## 2. Materials and procedure

The workpiece material used in the present work was carbon FRP laminates made from a commercial resin system of F593 prepregs with unidirectional carbon fibres of 7–8 $\mu$m in diameter. The prepregs were cured under the pressure of 0.6 MPa at the temperature of 177 °C for 2 h. The size of a laminate was 300 mm × 50 mm with a thickness of 4 mm, and the specimens used for grinding experiments featuring

* Corresponding author. Tel.: +61-2-9351-2835; fax: +61-2-9351-7060.
*E-mail address:* zhang@aeromech.usyd.edu.au (L.C. Zhang).

Table 1
Mechanical properties of the FRP material at room temperature

| Mechanical property | Value |
| --- | --- |
| Tensile strength (MPa) | 1331 |
| Tensile modulus (GPa) | 120 |
| Compressive strength (MPa) | 1655 |
| Compressive modulus (GPa) | 115 |
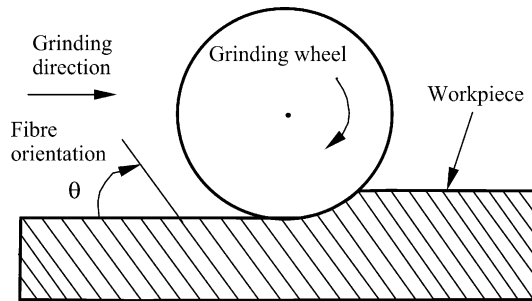


Fig. 1. Definitions of some grinding parameters.



Fig. 2. Effect of the fibre orientation on the grinding and cutting forces: (a) horizontal force and (b) vertical force.

$45 \times 15 \times 4$ (length × width × thickness, mm) were cut from the laminate with required fibre orientations. The mechanical properties of the workpiece material are listed in Table 1.

The tests were carried out by dry down-grinding as shown in Fig. 1 with an alumina wheel, BWA36HVAA, on a MININI M286 CN surface grinder. The grinding forces were measured with a three-dimensional piezoelectric dynamometer (Kistler 5011) mounted on the hydraulic table of the grinder. The grinding wheel was dressed regularly with a single point diamond dresser. The dressing depth was 0.1 mm each time. The dressing feed rate was 200 mm/min and the peripheral speed of the wheel was 20 m/s.
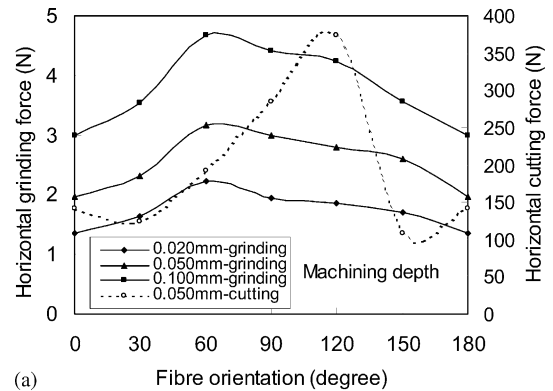
The velocities of the wheel and table were fixed at 25 m/s and 4 m/min, respectively. The fibre orientation $\theta$ was defined clockwise from the ground surface to the fibre direction as shown in Fig. 1. In the present study, $\theta$ was taken as $0°$, $30°$, $60°$, $90°$, $120°$ and $150°$, respectively, and the depth of grinding, $d$, was 20, 50, 100, 150 and 200 μm, respectively.
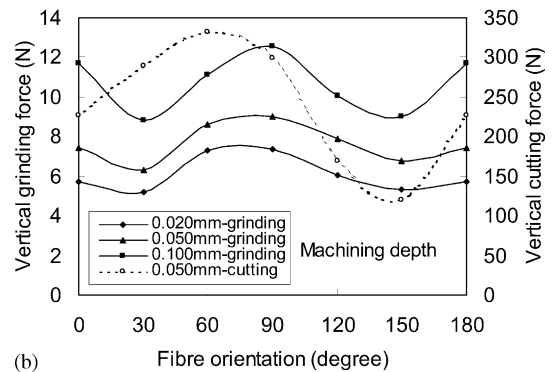
## 3. Results and discussion

### 3.1. Grinding force

Two orthogonal components of the grinding force were measured, i.e., the horizontal force parallel to the grinding direction and the vertical force perpendicular to the grinding surface. Fig. 2 shows the force variation with respect to the fibre orientation under different grinding depths. It is clear that both $\theta$ and $d$ contribute to the force generation.

Fig. 2(a) indicates that the horizontal grinding force increases when $\theta$ rises from $0°$ to $60°$, but drops afterward. This is determined by the deformation mechanism of the FRP. When $\theta = 0°$, the material removal was mainly caused by mode II shearing fracture and mode I opening cracking

along the fibre/matrix interfaces as illustrated in Fig. 3(a). As the fibre-matrix bonding strength is much lower than the fibre strength, the force needed to separate the fibre/matrix interfaces is also lower. With increasing the $\theta$, the material removal will involve the shearing fracture of the fibres, as shown in Fig. 3(b) and (c). Since the fibres have a high shearing strength, the grinding force goes up. At $\theta = 60°$, the horizontal grinding force reaches the maximum, while the maximum horizontal force occurs at $\theta = 90–120°$ in cutting. As recognised, both cutting force and grinding force depend dominantly on the material removal mechanisms (or fracture mechanisms of the material) in the machining process. In grinding at $\theta = 60°$, the material removal (or the fracture of fibres) consists of a large amount of pull-out and breakage of fibres, as well as shearing fracture of fibres, all these mechanisms contribute to the maximum grinding force. In orthogonal cutting at $\theta = 90°$, the material was removed by the mechanism of shearing fracture of fibres, and cutting a bundle of well-bonded fibres by the tool in the perpendicular direction (i.e., $\theta = 90°$) should have the largest resistance than other directions, just like a crack growing across a bundle of well-bonded fibres, which would meet the largest resistance. The largest vertical grinding force occurs at $\theta = 90°$, as shown in Fig. 2(b). This is because the fibres have the highest longitudinal strength and hence the resistance to the vertical compression of the grinding wheel
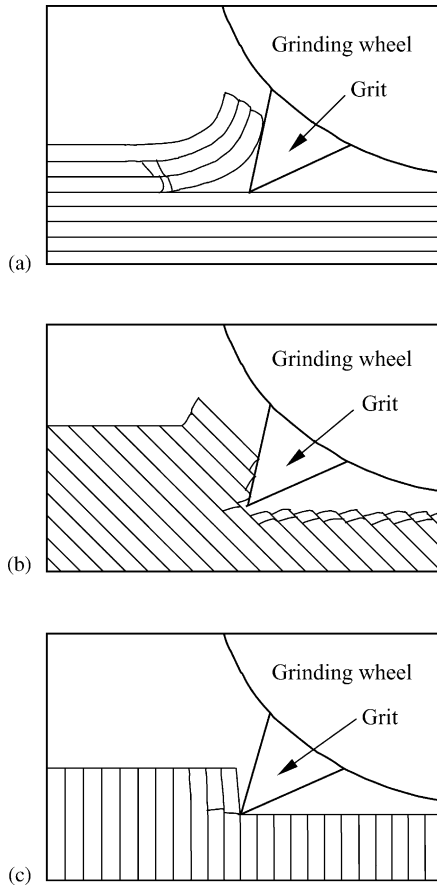
Fig. 3. Grinding mechanism of FRP materials: (a) $\theta = 0°$, (b) $\theta = 30$–$60°$, (c) $\theta = 90°$.



Fig. 4. Effect of the fibre orientation on surface roughness: (a) along the grinding direction and (b) perpendicular to the grinding direction.

becomes high when $\theta$ changes to $90°$. It is reasonable to observe that the vertical grinding force curves in Fig. 2(b) are not symmetric about $\theta = 90°$, because of the variation of the material removal mechanisms when $\theta$ varies.

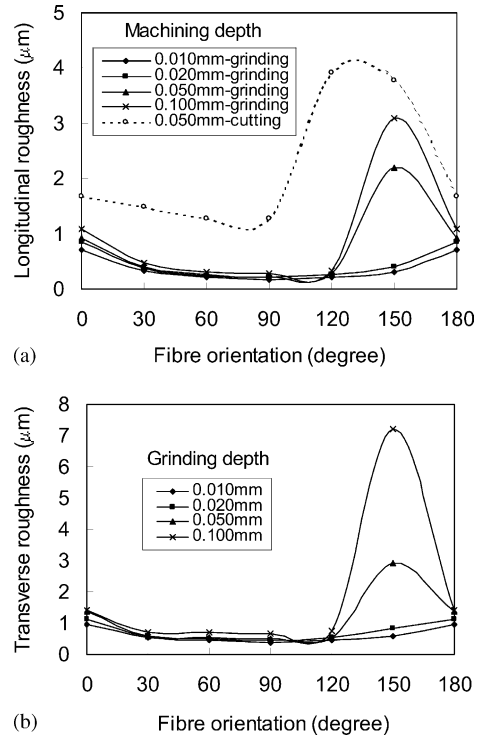The experimental results of grinding forces were compared with those of an orthogonal cutting for the same material [12,14], as shown in Fig. 2. In orthogonal cutting, the tool used was made from tungsten carbide with a clearance angle of $7°$ and a rake angle of $-20°$, and the cutting speed was fixed at 1 m/min. From Fig. 2, it is clear that the cutting forces vary in a different manner and they are much higher than grinding forces under the same nominal depths of cut. This is mainly because the cutting is a single point machining process with a constant rake angle, and the material removal mechanism was the fracture and separation of the bulk materials in front of the cutting tool edge, thus
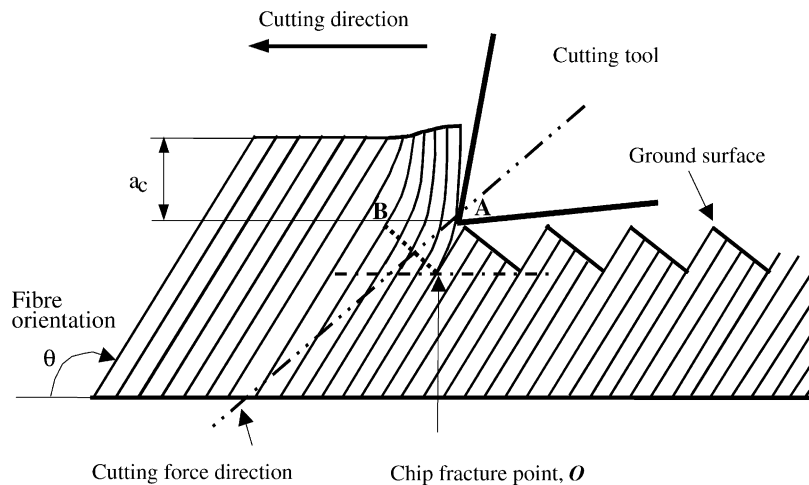


Fig. 5. Surface morphology formation when $\theta > 90°$.

resulting in a higher cutting force; while a grinding is a multipoint micro-machining process whose active abrasive grains have much smaller depths of cut and random rake angles (generally, the rake angles of abrasive grains are negative). Moreover, the differences between orthogonal cutting and grinding are also presented by the fact that the orthogonal cutting speed is very low (i.e., 1 m/min), thus the material removal rate per unit time is very high compared to the grinding which has a much higher peripheral speed of the grinding wheel (i.e., 20 m/s) and correspondingly a much lower material removal rate.

### 3.2. Surface roughness

Fibre orientation has a big influence on the surface roughness of ground specimens. Fig. 4 shows the relationship between the surface roughness and fibre orientation, where the longitudinal and transverse roughness were measured along and perpendicular to the grinding direction, respectively. For comparison, the surface roughness of specimens by orthogonal cutting [12] with the cutting depth of 50 μm and the rake angle of −20° is also presented in Fig. 4(a).

It is clear that there is a threshold of fibre orientation, $\theta = 120°$, below which the effect of $\theta$ is negligible. The best surface roughness is obtained at $\theta = 90–120°$ and the worst occurs at $\theta = 150°$. Orthogonal cutting gives similar results but the threshold is $\theta = 90°$ and the worst surface roughness happens at $\theta = 120–150°$ [12–14]. This is probably due to the effect of rake angles, because in grinding the rake angles of the active abrasive grains vary from −15° to −60° according to the literature [18,19].

The mechanism of the greater surface roughness, when $90° \leq \theta < 180°$, is illustrated qualitatively in Fig. 5. In orthogonal cutting, the composite ahead of the cutting tool bends and the interlaminar separation occurs along the fibre/matrix interface (i.e. along tool tip A to chip fracture point O). As long as the maximum bending stress at a certain point below the tool tip (e.g. point O) reaches the bending strength of the composite, fibre fracture happens at the point along direction OB which is mostly perpendicular to the fibres. Because point O is quite below the cutting edge, a rougher surface and a deeper damage penetration appear. This is quite different from the case when $0° \leq \theta < 90°$ at which fibres are under pulling and thus break in the very vicinity of the cutting edge. This was confirmed by the authors' high-speed camera observation and was in agreement with the report of [6,7]. Therefore, when grinding is viewed as a multipoint cutting process that has a myriad of micro-cutting edges with different rake angles, the greater variation of surface roughness with $\theta > 120°$ is not unexpectable.
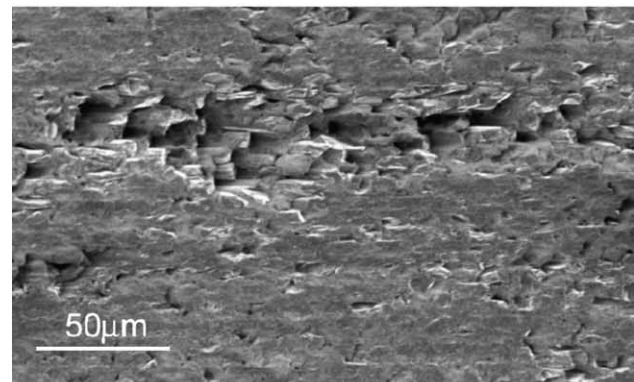
Moreover, under a relatively small depth of grinding close to the diameter of the carbon fibres, such as 10 and 20 μm, the effect of fibre orientation becomes trivial and the worst surface finish occurs at $\theta = 0°$. This is because at such a small depth of grinding, an abrasive cutting edge does not
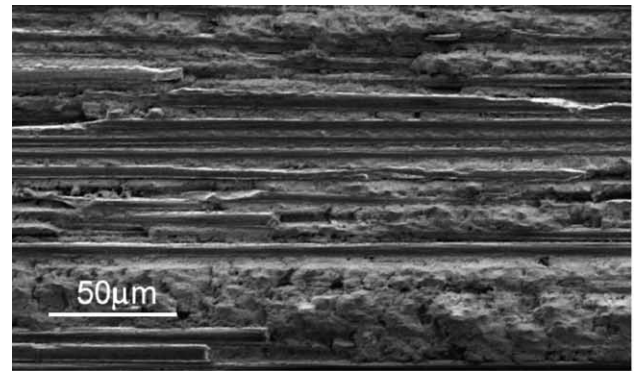


(a)
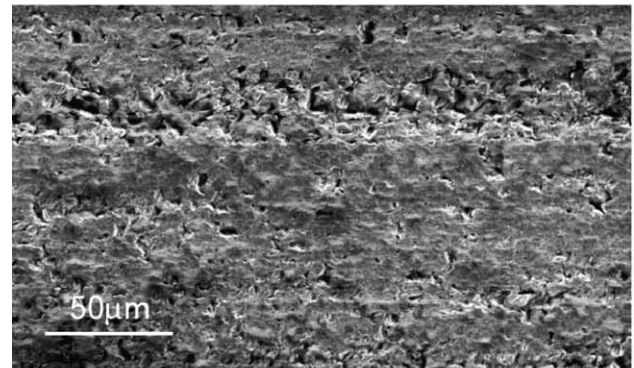


(b)



(c)

Fig. 6. SEM micrographs of ground surface at different fibre orientations ($d = 20$ μm): (a) $\theta = 0°$, (b) $\theta = 90°$, (c) $\theta = 150°$.

bring about much fibre-bending. Fibres do not fracture by cutting but debond at the fibre/matrix interfaces to create a rougher surface. A typical morphology of the ground surface of $\theta = 0°$ is shown in Fig. 6(a), where some arc-shaped grooves originally occupied by the fibres can be seen clearly.

### 3.3. Damage

As shown in Fig. 6, grinding introduced moderate damages when the depth of grinding is relatively small. This is consistent with the results of surface roughness.
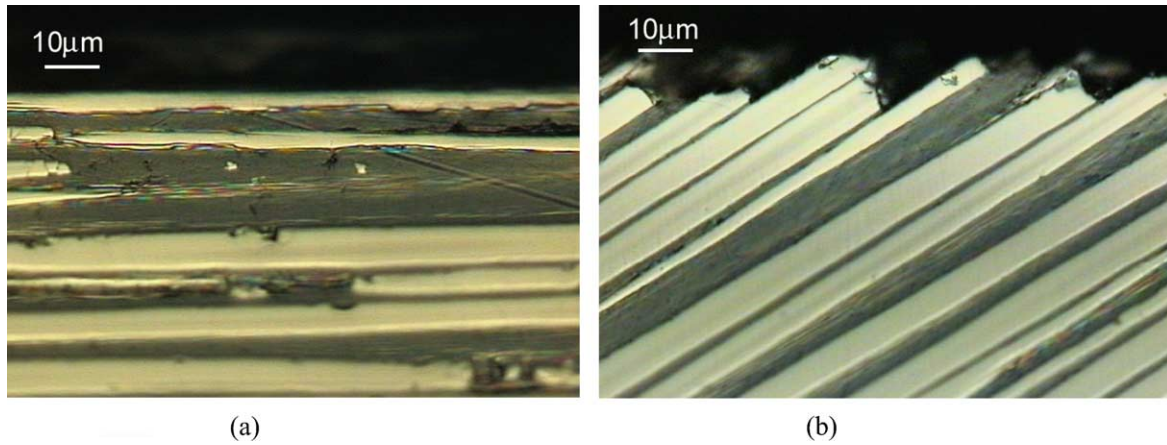
Fig. 7. Cross-sections of ground surfaces at different fibre orientations ($d = 20\,\mu$m): (a) $\theta = 0°$ and (b) $\theta = 150°$.
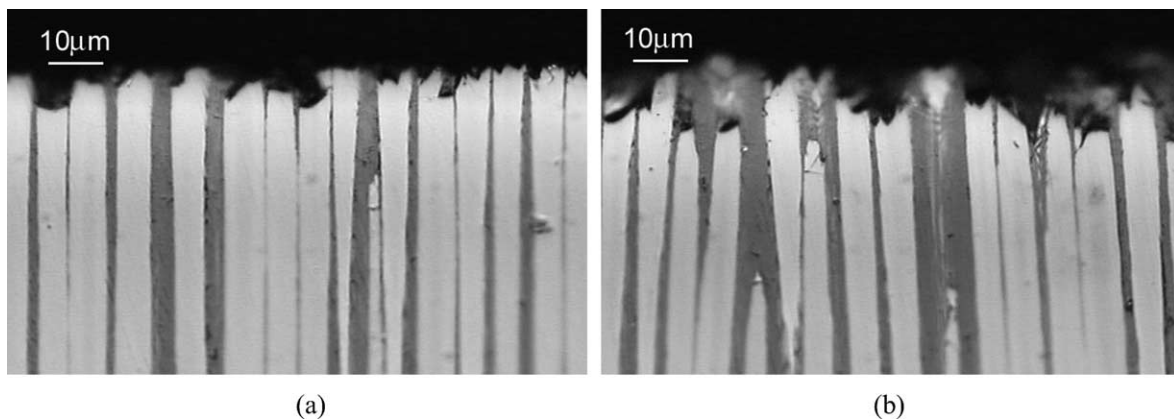


Fig. 8. Cross-sections of ground surfaces at different grinding depths ($\theta = 90°$): (a) $d = 20\,\mu$m and (b) $d = 100\,\mu$m.

As indicated in Fig. 4, surface roughness reaches its maximum at $\theta = 150°$. This is also shown by the SEM observations in Figs. 6 and 7. There are some severe damages on the ground surfaces and the degree of damage increases with the depth of grinding.

Fig. 7 shows the cross-section views under a Leica optical microscope when $\theta = 0°$ and $150°$ and $d = 20\,\mu$m. It can be seen that with $\theta = 0°$ the surface layer contains obvious microcracks along interfaces of fibre/matrix, i.e., some delaminations occur. This is apparently caused by the large shear force along the interfaces. When $\theta = 150°$, a saw-toothed shape appears, which is in good agreement with the machining mechanism illustrated in Fig. 5 and the large surface roughness shown in Fig. 4 ($120° < \theta < 180°$). Fig. 8 manifests the cross-sectional observations at different grinding depths when $\theta = 90°$. It is clear that the damage-affected zone expands when the grinding depth increases.

## 4. Conclusions

(1) Chip formation, grinding forces and surface integrity in grinding of an FRP with unidirectional fibres are highly dependent on fibre orientations.

(2) The fibre orientation of $90°$ gives rise to the lowest surface roughness, and the grinding depth has less effect on the surface roughness. A fibre orientation between $120°$ and $180°$ is not favourable, which can lead to a saw-toothed surface morphology and deep subsurface damage.

(3) The depth of the damage-affected zone increases with the increment of grinding depth for all the fibre orientations studied.

## Acknowledgements

## References

[1] W. König, Ch. Wulf, P. Grass, H. Willerscheid, Machining of fibre-reinforced plastics, Ann. CIRP 34 (2) (1985) 537–548.
[2] A. Koplev, Aa. Lystrup, T. Vorm, The cutting process, chips, and cutting forces in machining CFRP, Composites 14 (1983) 371–376.

[3] H. Inoue, M. Ido, Study on the cutting mechanism of GFRP, in: Proceedings of International Symposium on Composite Materials and Structures, June 10–13, 1986, Beijing, China, pp. 1110–1115.

[4] T. Kaneeda, CFRP cutting mechanism, Trans. N. Am. Manuf. Res. Inst. SME 19 (1991) 216–221.

[5] N. Bhatnagar, N. Ramakrishnan, N.K. Naik, R. Komanduri, On the machining of fibre-reinforced plastic (FRP) composite laminates, Int. J. Mach. Tools Manuf. 35 (1995) 701–716.

[6] D.H. Wang, M. Ramulu, D. Arola, Orthogonal cutting mechanisms of graphite/epoxy composite, Part I, Unidirectional laminate, Int. J. Mach. Tools Manuf. 35 (1995) 1623–1638.

[7] D.H. Wang, M. Ramulu, D. Arola, Orthogonal cutting mechanisms of graphite/epoxy composite, Part II, Multi-directional laminate, Int. J. Mach. Tools Manuf. 35 (1995) 1639–1648.

[8] V. Tagliaferri, G. Caprino, A. Diterlizzi, Effect of drilling parameters on the finish and mechanical properties of GFRP composites, Int. J. Mach. Tools Manuf. 30 (1990) 77–84.

[9] G. Caprino, V. Tagliaferri, Damage development in drilling glass fibre-reinforced plastics, Int. J. Mach. Tools Manuf. 35 (1995) 817–829.

[10] H. Inoue, I. Kawaguchi, Study on the grinding mechanism of glass fibre-reinforced plastics, J. Eng. Mater. Technol., Trans. ASME 112 (1990) 341–345.

[11] K.Y. Park, D.G. Lee, T. Nakagawa, Mirror surface grinding characteristics and mechanism of carbon fibre-reinforced plastics, J. Mater. Process. Technol. 52 (1995) 386–398.

[12] X.M. Wang, L.C. Zhang, Machining damage in unidirectional fibre-reinforced plastics, in: Abrasive Technology: Current Development and Applications I, World Scientific, Singapore, 1999, pp. 429–436.

[13] L.C. Zhang, H.Y. Zhang, X.M. Wang, A force prediction model for cutting unidirectional fibre-reinforced plastics, Mach. Sci. Technol. 5 (2001) 293–305.

[14] X.M. Wang, L.C. Zhang, An experimental investigation into the orthogonal cutting of unidirectional fibre-reinforced plastics, Int. J. Mach. Tools Manuf. 43 (2003) 1015–1022.

[15] M. Mahdi, L.C. Zhang, An adaptive three-dimensional finite element algorithm for the orthogonal cutting of composite materials, J. Mater. Process. Technol. 113 (2001) 368–372.

[16] M. Mahdi, L.C. Zhang, A finite element model for the orthogonal cutting of fibre-reinforced composite materials, J. Mater. Process. Technol. 113 (2001) 373–377.

[17] H.J. Zhang, W.Y. Chen, D.C. Chen, L.C. Zhang, Assessment of the exit defects in carbon fibre-reinforced plastic plates caused by drilling, Precis. Mach. Adv. Mater., Key Eng. Mater. 196 (2001) 43–52 (special issue).

[18] S. Markin, Grinding technology—theory and applications of machining with abrasives, Ellis Horwood Limited, Chichester, 1989.

[19] M.C. Shaw, Principles of the Abrasive Processing, Clarendon press, Oxford, 1996.